Spectral and electro-optic response of UV-written waveguides in $LiNbO_3$ single crystals

C.L. Sones[1]*, P. Ganguly[1,3], Y.J. Ying[1], F. Johann[2], E. Soergel[2], R.W. Eason[1], and S. Mailis[1]

[1]*Optoelectronics Research Centre, University of Southampton, Southampton, SO17 1BJ, U.K.*
[2]*Institute of Physics, University of Bonn, Wegelerstrasse 8, 53115 Bonn, Germany.*
[3]*On leave from Advanced Technology Development Centre, Indian Institute of Technology, Kharagpur, 721302, India.*
*cls@orc.soton.ac.uk

Abstract: An experimental study of the spectral and electro-optic response of direct UV-written waveguides in $LiNbO_3$ is reported. The waveguides were written using c.w. laser radiation at 275, 300.3, 302, and 305 nm wavelengths with various writing powers (35-60 mW) and scan speeds (0.1-1.0 mm/sec). Spectral analysis was used to determine the multimode and single mode wavelength regions and, the cut-off point of the fabricated waveguides. Electro-optic characterization of these waveguides reveals that the electro-optic coefficient (r_{33}) decreases for longer writing wavelengths, with a maximum of 31 pm/V for 275 nm and, is reduced to 14 pm/V for waveguides written with 305 nm.

OCIS codes: (130.3730) Lithium niobate; (130.3130) Integrated optics materials; (130.3120) Integrated optics devices; (130.2790) Guided waves.

References and links

1. S. Mailis, C. Riziotis, I. T. Wellington, P. G. R. Smith, C. B. E. Gawith, and R. W. Eason, "Direct ultraviolet writing of channel waveguides in congruent lithium niobate single crystals," Opt. Lett. **28**(16), 1433–1435 (2003).
2. P. Ganguly, C. L. Sones, Y. J. Ying, H. Steigerwald, K. Buse, E. Soergel, R. W. Eason, and S. Mailis, "Determination of Refractive Indices From the Mode Profiles of UV-Written Channel Waveguides in $LiNbO_3$-Crystals for Optimization of Writing Conditions," J. Lightwave Technol. **27**(16), 3490–3497 (2009).
3. A. C. Muir, G. J. Daniell, C. P. Please, I. T. Wellington, S. Mailis, and R. W. Eason, "Modelling the formation of optical waveguides produced in $LiNbO_3$ by laser induced thermal diffusion of lithium ions," Appl. Phys., A Mater. Sci. Process. **83**(3), 389–396 (2006).
4. K. A. H. van Leeuwen, and H. T. Nijnuis, "Measurement of higher-order mode attenuation in single-mode fibers: effective cutoff wavelength," Opt. Lett. **9**(6), 252–254 (1984).
5. T. Lang, L. Thevenaz, Z. B. Ren, and P. Robert, "Cutoff wavelength measurement of $TiLiNbO_3$ channel waveguides," Meas. Sci. Technol. **5**(9), 1124–1130 (1994).
6. P. Ganguly, B. Umapathi, S. Das, J. C. Biswas, and S. K. Lahiri, "Fabrication and characterisation of Ti:$LiNbO_3$ waveguides," in *International conference on Optics and Optoelectronics* (Dehradun, India, 9–12th December, 1998), pp. 450–455.
7. C. F. McConaghy, K. F. Hunenberg, D. Sweider, M. Lowry, and R. A. Becker, "White-light spectral-analysis of Lithium-Niobate wave-guides," J. Lightwave Technol. **13**(1), 83–87 (1995).
8. A. Mendez, G. De la Paliza, A. Garcia-Cabanes, and J. M. Cabrera, "Comparison of the electro-optic coefficient (r_{33}) in well-defined phases of proton exchanged $LiNbO_3$ waveguides," Appl. Phys. B **73**, 485–488 (2001).
9. S. Ducharme, J. Feinberg, and R. R. Neurgaonkar, "Electrooptic and piezoelectric measurements in photorefractive Barium Titanate and Strontium Barium Niobate," IEEE J. Quantum Electron. **23**(12), 2116–2121 (1987).
10. E. L. Wooten, and W. S. C. Chang, "Test structures for characterization of electrooptic waveguide modulators in lithium niobate," IEEE J. Quantum Electron. **29**(1), 161–170 (1993).
11. A. Ródenas, D. Jaque, C. Molpeceres, S. Lauzurica, J. L. Ocana, G. A. Torchia, and F. Agullo-Rueda, "Ultraviolet nanosecond laser-assisted micro-modifications in lithium niobate monitored by Nd^{3+} luminescence," Appl. Phys., A Mater. Sci. Process. **87**(1), 87–90 (2007).
12. D. C. Deshpande, A. P. Malshe, E. A. Stach, V. Radmilovic, D. Alexander, D. Doerr, and D. Hirt, "Investigation of femtosecond laser assisted nano and microscale modifications in lithium niobate," J. Appl. Phys. **97**(7), 074316 (2005).

#117228 - $15.00 USD Received 14 Sep 2009; revised 3 Nov 2009; accepted 3 Nov 2009; published 11 Dec 2009

13. J. Burghoff, C. Grebing, S. Nolte, and A. Tunnermann, "Waveguides in lithium niobate fabricated by focused ultrashort laser pulses," Appl. Surf. Sci. **253**(19), 7899–7902 (2007).
14. H. Nishihara, M. Haruna, and T. Suhara, *Optical Integrated Circuits* (McGraw-Hill, New York, 1989).
15. I. P. Kaminow, and V. Ramaswam, "Lithium-Niobate ridge waveguide-modulator," Appl. Phys. Lett. **24**(12), 622–624 (1974).
16. A. C. Muir, C. L. Sones, S. Mailis, R. W. Eason, T. Jungk, A. Hoffman, and E. Soergel, "Direct-writing of inverted domains in lithium niobate using a continuous wave ultra violet laser," Opt. Express **16**(4), 2336–2350 (2008).
17. F. Johann, Y. J. J. Ying, T. Jungk, A. Hoffmann, C. L. Sones, R. W. Eason, S. Mailis, and E. Soergel, "Depth resolution of piezoresponse force microscopy," Appl. Phys. Lett. **94**(17), 172904 (2009).
18. J. A. de Toro, M. D. Serrano, A. G. Cabanes, and J. M. Cabrera, "Accurate interferometric measurement of electro-optic coefficients: application to quasi-stoichiometric $LiNbO_3$," Opt. Commun. **154**(1-3), 23–27 (1998).

1. Introduction

Since its inception, the UV directly written waveguide [1] procedure in lithium niobate ($LiNbO_3$) single crystals has held considerable promise because it is a single-step process which is well suited for complex micro-optical devices, in addition to conventional optical integrated circuits. Direct writing of graded-index channel waveguides in congruent $LiNbO_3$ has been demonstrated using c.w. laser light within a writing wavelength range of 244 – 305 nm [1,2]. The process has been modeled as a laser-induced thermal diffusion of lithium ions which results in a variation of the local Li concentration which increases the extra-ordinary refractive index of $LiNbO_3$ [2,3] For most applications, single-mode waveguides are essential in order to achieve optimised device performance, and hence the determination of single-mode operating range and cut-off wavelength of the waveguide are fundamental for characterising waveguide optical properties. Spectral analysis is a characterization method which has been originally developed for determining the effective cut-off wavelength of optical fiber [4] and later for Ti-indiffused [5,6] and proton exchanged [7] waveguides, and this may also be applied to these UV-written waveguides. Moreover, the electro-optic properties of these waveguides need to be assessed for subsequent applications in waveguide optical switches and modulators, which are key integrated-optical components that can be implemented in $LiNbO_3$. Therefore, spectral analysis and electro-optic characterisation of UV-written waveguides in $LiNbO_3$ are of absolute necessity from the device point of view.

In this paper a white light laser-continuum source has been used for the investigation of the spectral response of the direct UV-written channel waveguides in congruent $LiNbO_3$. The spectral data was used to determine the various regimes of waveguide operation from multimode to cut-off. It has been observed that an optimum writing condition for these waveguides exists where the refractive index change is maximised and hence the cut-off wavelength of the waveguide shifts to longer wavelengths. The experimental study was extended to the electro-optic properties of these waveguides, which reveals that electro-optic response of the waveguide reduces with increasing recording wavelength, with 275 nm written waveguides having the highest electro-optic response compared to waveguides written with 300.3, 302, and 305 nm light. Measurements of mode-width, mode-depth, and refractive-index change of waveguides with various applied voltages, and finally direct interferometric measurements of the electro-optic coefficient of waveguides written at different UV wavelengths have confirmed this experimental finding.

2. Experimental

2.1. Waveguide fabrication

Direct writing of waveguides in congruent, z-cut $LiNbO_3$ crystal has been achieved using an argon ion laser that yields c.w. output at 275, 300.3, 302, and 305 nm wavelengths. The laser beam was focused onto the crystal surface to a spot of ~4 μm diameter. The waveguides were written on the + z face of the crystal, along the crystallographic y-direction, by scanning the crystal in front of the focussed laser beam using a computer-controlled 2D translation stage. The laser power and scanning speed used in our experiments were within the range of 35-60 mW and 0.1-1.0 mm/sec, respectively, which correspond to UV energy fluences of 0.7-12.0 kJ/cm^2. The strong optical absorption of $LiNbO_3$ at these ultraviolet wavelengths results in an

#117228 - $15.00 USD Received 14 Sep 2009; revised 3 Nov 2009; accepted 3 Nov 2009; published 11 Dec 2009

increased local temperature- that induces Li diffusion takes place which forms the waveguides with an increased extra-ordinary index of refraction [1–3]. While the waveguides were in most cases free from surface damage, those written at the higher end of the energy fluence range did exhibit some undesirable surface damage. Following the direct writing, all the waveguides were edge-polished and used for the subsequent spectral and electro-optic characterization.

2.2. Spectral measurements

A supercontinuum fiber laser (Fianium, Femtopower 1060, with a wavelength range: 408 – 1800 nm) was coupled into the waveguides using a 10x microscope objective. The output of each waveguide was imaged by a second microscope objective onto a circular aperture (iris diaphragm) for spatially filtering out the optical noise from the light originating from the waveguides. This was subsequently then coupled to an optical spectrum analyzer. A schematic of the experimental setup is shown in Fig. 1. The numerical aperture of the launching objective lens (NA = 0.25) was chosen to be high enough to excite all possible guided modes of the waveguides. The length of the channel waveguides used in our experiments was 14 mm. The $LiNbO_3$ substrate containing the waveguides was mounted onto a high precision 4-axis translation stage. TM waveguide modes only could be excited in these UV-written waveguides indicative of an increment only in the extra-ordinary refractive index. To eliminate the spectral response of the launch and detection components of the experimental setup (such as the broadband source and the detector), the spectral output intensity of the waveguide (I_{WG}) was normalized by a reference intensity spectrum (I_{REF}) acquired by the optical system without the presence of the waveguide. This normalization also minimizes the effect of chromatic aberrations of the microscope lenses. All these spectral measurements were performed below the photorefractive damage threshold of the waveguides, which was confirmed by the non-dependency of the normalized transmission spectra on the input power. The measured spectral response has been analyzed to determine the wavelength range for multi-mode and single-mode operation respectively and the cut-off wavelength of the UV-written waveguides.

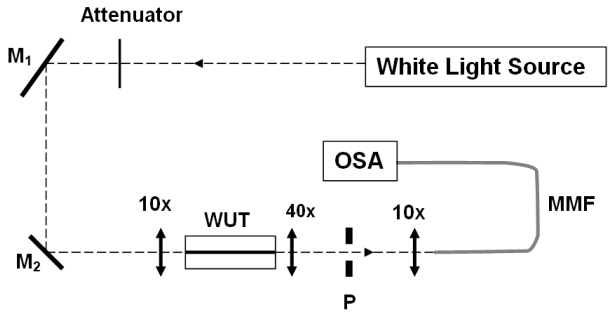

Fig. 1. Experimental setup for spectral characterisation: M_1, M_2 – mirrors, P – adjustable pinhole, MMF – multimode fiber, OSA – optical spectrum analyser, WUT – waveguide under test.

The change of the spectral response of the UV-written waveguides under the influence of an external electric field was used to investigate the electro-optic behavior of the waveguides. A pair of thin gold film electrodes of thicknesses ~10 nm was sputtered onto the two opposite faces of the 500 μm thick substrate containing the waveguides. The electrodes were used to apply a variable voltage across the substrate and the corresponding normalized transmission spectra of the waveguides were measured. The applied dc voltage used in our experiment ranged from −600 to + 600 V, corresponding to a uniformly applied dc electric field ranging from −1.2 to + 1.2 V/μm along the z-axis of the $LiNbO_3$ crystal. The changes in cut-off wavelengths of the waveguides, written with different wavelengths, for various applied voltages were measured. These experimental data directly correspond to the relative refractive

#117228 - $15.00 USD Received 14 Sep 2009; revised 3 Nov 2009; accepted 3 Nov 2009; published 11 Dec 2009

index changes or changes in the contrast of the waveguides with respect to the substrate, via the linear electro-optic (Pockels) effect. The markedly different responses of the waveguides with applied voltage suggest a difference in the relative values of electro-optic coefficient (r_{33}) of the UV-written waveguides compared to those for the bulk substrate under different writing wavelengths. Hence it was necessary to proceed to a direct measurement of the effective electro-optic coefficient.

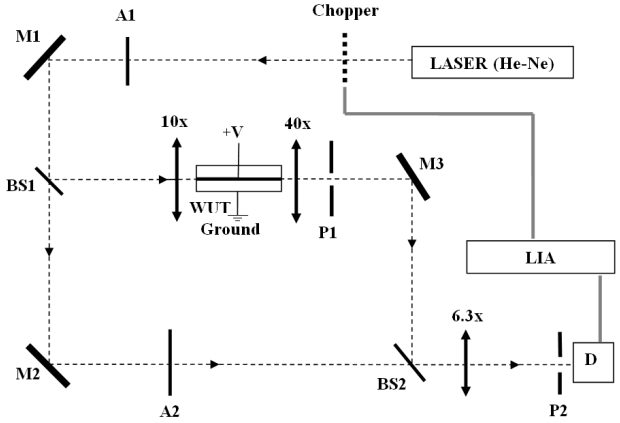

Fig. 2. Experimental setup for the measurement of electro-optic coefficient of the waveguide: A1, A2 – optical attenuator; M1, M2, M3 – mirror; BS1, BS2 – beam splitter; WUT – waveguide under test; V - applied voltage; P1, P2, - adjustable pinhole; D – detector; LIA – lock-in amplifier.

2.3. Electro-optic coefficient measurement

For a quantitative characterization of the electro-optic response of the waveguides written at different wavelengths, we measured the r_{33} electro-optic coefficient using a Mach-Zehnder interferometer setup, a schematic of which is shown in Fig. 2. A He-Ne laser beam (0.6328 μm) was divided by a 50/50 cube beam- splitter into the two arms of the interferometer. The waveguide under test was placed in one arm of the interferometer, and light was in- and out-coupled using microscope objectives. In the reference arm a variable attenuator was placed to balance the optical power between the two arms of the interferometer. Finally the beams from the two arms were recombined using a second cube beam-splitter as shown in the schematic. The polarization of the input light was made parallel to the z-axis of the crystal. Initially a computer-interfaced CCD camera was used to observe the series of elliptical interference fringes at the output. A pinhole with diameter ~25 μm was used to sample the interference fringes and to enable the detection of phase shifts as a variation of the transmitted optical power measured by a Si photo-detector. An optical chopper (frequency: 170 Hz) in conjunction with a lock-in-amplifier was used to improve the signal-to-noise ratio (typically ~50) of our detection system. We also placed a 6.3x microscope objective to magnify the output interference pattern and hence improve the resolution of the pinhole-detector assembly. The entire experimental setup was on a vibration-isolated table and the interferometric section was covered to minimize the effect of random phase changes caused by air-flow in the two arms of the interferometer. The applied voltage introduces a refractive index change in the waveguide via the electro-optic effect thereby introducing a phase difference between the two arms of the interferometer. This small phase difference produces a spatial shift in the interference fringes, and hence a change in detector output. From the plot of the detector output versus the applied voltage, we have measured the half-wave voltage V_{π}, the voltage required to produce a π-phase shift. This is related to the r_{33} coefficient of the waveguide by the following equation [8,9]

#117228 - $15.00 USD Received 14 Sep 2009; revised 3 Nov 2009; accepted 3 Nov 2009; published 11 Dec 2009

$$r_{33} = \frac{\lambda d}{n_e^3 L V_{\Pi}} \tag{1}$$

where, λ is the operating wavelength (0.6328 μm), d is the substrate thickness (500 μm), n_e is the effective refractive index of the waveguide, and L is the length of the electrode-covered waveguide section (9 mm). In Eq. (1) we have assumed 100% overlapping of the applied electric field with the waveguide propagation mode which is a valid approximation in the present configuration [10]. The experiment was repeated for a number of waveguides written with different writing wavelengths and powers, and the r_{33} coefficient for each waveguide was determined by using Eq. (1). No phase drift due to optical "photorefractive" damage was observed over the duration of the measurements.

3. Results and discussions

3.1. Analysis of spectral data of the waveguides

Typical normalized transmission spectra of two different UV-written waveguides are shown in Fig. 3. The spectrum shown in Fig. 3(a) corresponds to a waveguide that exhibits multimode transmission at shorter wavelengths and can be divided into four regions [7]. In region-1 the waveguide supports the two lowest order modes and the normalized transmission spectrum (I_{WG}/I_{REF}) can be described as:

$$\frac{I_{WG}}{I_{REF}} = K_{00} + K_{01} \tag{2}$$

where K_{00} and K_{01} are the coupling coefficients for the lowest and next higher order modes, respectively. Region-2 describes the wavelength regime where the second mode cut-off is approached. In this case normalised transmission spectrum is given by:

$$\frac{I_{WG}}{I_{REF}} = K_{00} + K_{01} e^{-\alpha_{01} L_0} \tag{3}$$

where α_{01} and L_0 are the modal attenuation coefficient of the higher order mode and length of the guide, respectively. As the wavelength becomes longer the cut-off of the second mode is passed and region-3 covers the wavelength range where the fundamental mode is still far from cut-off. The intensity ratio in this region may be given as:

$$\frac{I_{WG}}{I_{REF}} = K_{00} \tag{4}$$

Finally as the fundamental mode cut-off is approached in region-4, the normalized transmission spectrum is:

$$\frac{I_{WG}}{I_{REF}} = K_{00} e^{-\alpha_{00} L_0} \tag{5}$$

where α_{00} is the attenuation coefficient for the fundamental mode. In Eqs. (2-5) the modal coupling and attenuation coefficients are wavelength dependent. We have defined 10% of the peak normalised intensity as the mode cut-off point. Hence for the waveguide shown in Fig. 3(a), which was written at the 300.3 nm wavelength, with a laser power of 40 mW and a scan speed 1.0 mm/sec, the multimode region is <514 nm, whereas the guide is single-moded within the wavelength range from 514 nm to 780 nm, where 780 nm is practically the waveguide cut-off wavelength. For the waveguide shown in Fig. 3(b), written with 305 nm wavelength, 50 mW power and 1 mm/sec laser scan speed, the single-mode range is from 408 nm to 615 nm.

#117228 - $15.00 USD Received 14 Sep 2009; revised 3 Nov 2009; accepted 3 Nov 2009; published 11 Dec 2009

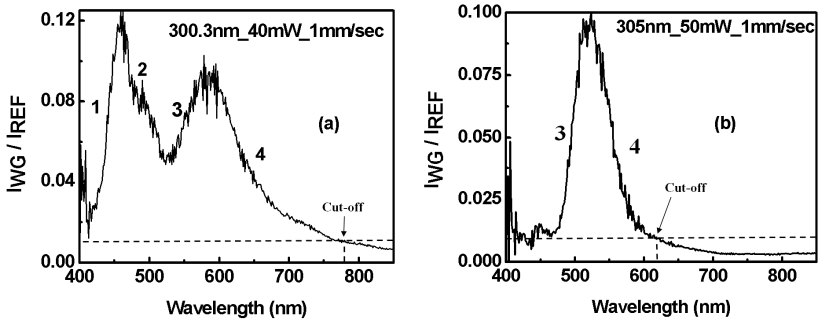

Fig. 3. Typical spectral responses of the fabricated UV-written waveguides: (a) with writing wavelength: 300.3 nm, power: 40 mW, speed: 1 mm/sec; (b) with writing wavelength: 305 nm, power: 50 mW, speed: 1 mm/sec.

We have measured the cut-off wavelengths of all the waveguides written with various writing wavelengths, laser powers, and scan speeds. The variations of the cut-off wavelength of the waveguides written with different wavelengths, as a function of laser power and scan speed are shown in Fig. 4(a) and Fig. 4(b) respectively.

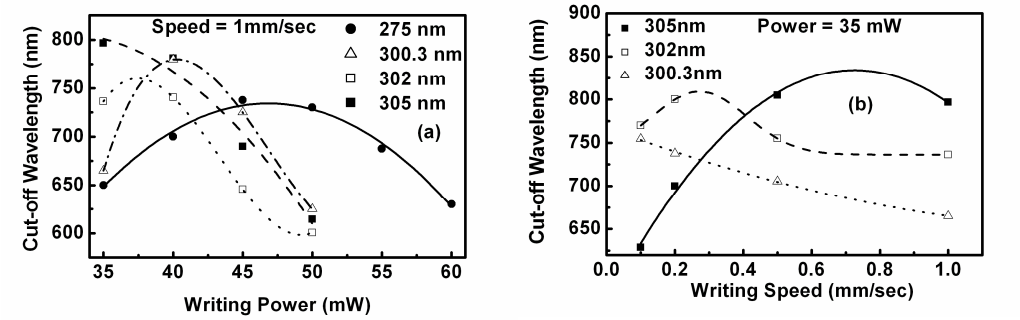

Fig. 4. Variations of cut-off wavelengths of the waveguides with: (a) laser writing power, (b) writing speed.

These results confirm our previous observation [2] that for each writing wavelength an optimum writing condition (writing power and scan speed) exists where the induced refractive index change is maximised. As the refractive index change or the contrast of the waveguide (Δn_{max}) increases, the cut-off shifts to longer wavelengths. This may be because of the trade-off between the laser-induced refractive index change and the strain due to surface damage of the waveguides at higher laser fluences. UV laser-induced surface damage has been investigated by Rodenas et al. in [11], where it was demonstrated that it induces a permanent local stress of micron-scale dimension, causing a decrease in local refractive index of $LiNbO_3$ to some extent [12]. Raman analysis of the exposed region also shows some loss of crystallinity of the material [13], indicating that though $LiNbO_3$ may suffer some change in chemical structure at the superficial surface layer, it remains largely unchanged in the bulk.

3.2. Spectral analysis with applied voltages

Results of the measurements for cut-off wavelength change with applied dc voltages of waveguides written with four different UV wavelengths are shown in the graph of Fig. 5.

#117228 - $15.00 USD Received 14 Sep 2009; revised 3 Nov 2009; accepted 3 Nov 2009; published 11 Dec 2009

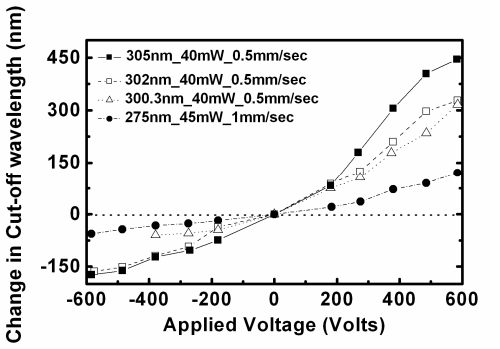

Fig. 5. Changes in cut-off wavelengths of the waveguides with applied voltages for 275, 300.3, 302, and 305 nm writing wavelengths.

It may be observed in the graph that the waveguides written with 275 nm exhibit the lowest change in cut-off wavelength with applied voltages in the range from −600 to + 600 V. The changes in cut-off wavelengths of the waveguides gradually increase with the writing wavelength. In the present electrode configuration, where a uniform electric field is applied across the whole crystal containing the waveguides, the change in cut-off wavelength will depend on the change in refractive index contrast of the waveguides with respect to the substrate. Hence for waveguides with the same electro-optic coefficients as that of $LiNbO_3$ substrate, there shouldn't be any appreciable change in the cut-off wavelength. However, waveguides which have a reduced electro-optic coefficient with respect to the substrate will exhibit a more significant change in cut-off wavelength with the applied voltage. Thus the results in Fig. 5 indicate that a waveguide written with 275 nm has an electro-optic coefficient, r_{33}, closest to the substrate value in comparison to waveguides written with longer wavelengths. In fact, the electro-optic coefficient decreases monotonically with the increase in writing wavelength. The measured change in contrast of these waveguides with respect to the substrate refractive index at 0.6328 μm transmitting wavelength (Fig. 6), for different applied voltages, supports these experimental observations. Maximum refractive index values near the surface for these waveguides without applying any voltages are given in Table 1.

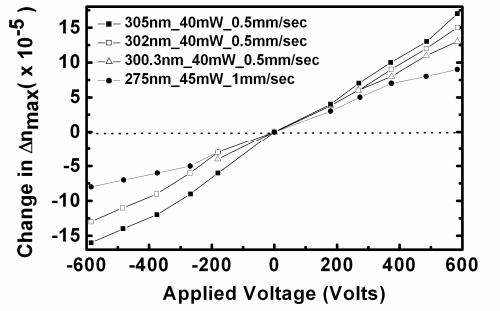

Fig. 6. Changes in contrast of the waveguides written with 275, 300.3, 302, and 305nm wavelengths with applied voltages.

Table 1. Maximum surface refractive index values of different waveguides in Fig. 6.

Laser Writing Wavelength (nm)	Laser Power (mW)	Scan Speed (mm/sec.)	Maximum Refractive Index Near Surface
275	45	1.0	2.204864
300.3	40	0.5	2.203554
302	40	0.5	2.204354
305	40	0.5	2.204154

#117228 - $15.00 USD Received 14 Sep 2009; revised 3 Nov 2009; accepted 3 Nov 2009; published 11 Dec 2009

The changes in mode width and mode depth of these UV-written waveguides with the applied voltages are shown in Fig. 7. The details of the experimental setup for mode profile measurement and determination of refractive index contrast of the waveguides are presented in Ganguly et al. [2]. All these waveguides are single-moded in nature at this wavelength within the applied voltage range. As expected the changes in mode widths and mode depths for the waveguide written with 275 nm wavelength with the applied voltages are relatively small, whereas, for other waveguides significant changes in mode widths and mode depths are observed. It may also be noted that the asymmetry in Fig. 5 for + ve and –ve applied voltages actually reflects the asymmetric behavior of mode depth variation of the waveguides as seen in Fig. 7(b). We have observed a measurable mode shrinkage or expansion along the applied electric field direction for these UV-written waveguides.

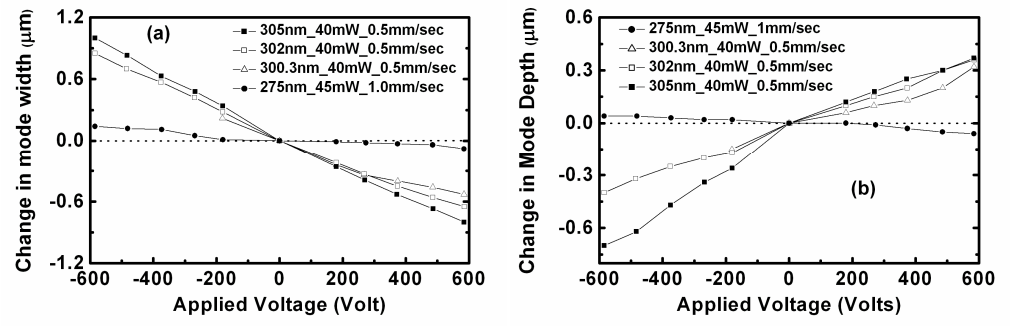

Fig. 7. Changes in mode width (a) and mode depth (b) with applied voltages for the waveguides written with 275, 300.3, 302, and 305nm wavelengths.

3.3. Electro-optic coefficients of the waveguides

The interferometrically measured electro-optic coefficient (r_{33}) of the waveguides written with these four different wavelengths and writing powers (45, 50, 55, 60 mW) are summarized in the graph shown in Fig. 8.

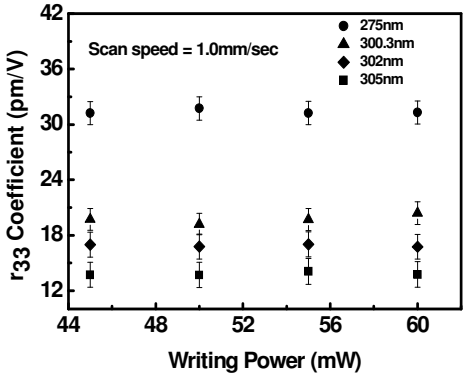

Fig. 8. Measured electro-optic coefficients (r_{33}) of the waveguides for different writing wavelengths and powers.

All the waveguides were written with a scanning speed of 1.0 mm/sec. Our measurements were performed with a dc applied field at room temperature (20 °C), for a probe wavelength of 0.6328 μm. Typical variations of normalised detector output with applied voltage are presented in Fig. 9, for the waveguides with different writing wavelengths. The non-zero minimum detector outputs may be a combined effect of slightly unequal intensity of the two arms of the interferometer under applied voltages and other stray environmental effects. It

#117228 - $15.00 USD Received 14 Sep 2009; revised 3 Nov 2009; accepted 3 Nov 2009; published 11 Dec 2009

may be concluded from these results that the electro-optic coefficient is as low as 14 pm/V for waveguides written with 305 nm wavelength, but increases with decreasing writing wavelength, to a value (31 pm/V) that is close to the bulk r_{33} value of the crystal, for 275 nm writing wavelength. It may also be noticed that the electro-optic coefficients of the waveguides are effectively independent of the writing laser powers within our studied experimental range. For comparison we have also measured the r_{33} coefficient of a Ti-indiffused channel waveguide fabricated in our laboratory, using the same experimental apparatus. The measured value of 35 pm/V is ~13% higher than the values for waveguides written with 275 nm wavelength. We also studied the a.c. (upto 10 KHz) electro-optic response of the waveguides using the same interferometric setup. A dc bias (0-100V) was also applied along with the sinusoidal ac signal (V_{pp} = 35-155 V) to set the phase difference between the interferometer arms to π/2, effectively increasing the detection sensitivity. It was observed that within the studied frequency range the frequency response of the UV-written waveguides is similar to that of the Ti-indiffused waveguide.

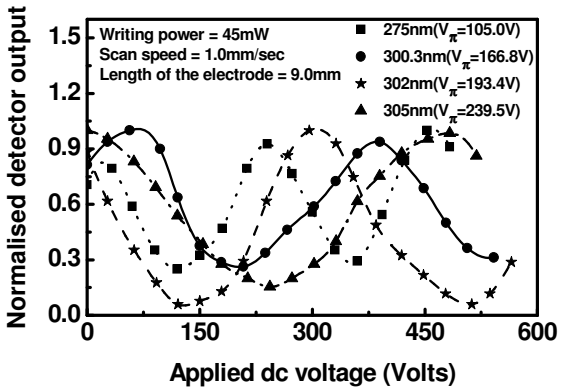

Fig. 9. Variation of normalised detector output with the applied voltages for 275, 300.3, 302, and 305nm writing wavelengths of the waveguides.

The reason for the electro-optic coefficient reduction at 300.3, 302, and 305 nm writing wavelengths, is not clearly understood at the moment. Since lithium out-diffused waveguides are known to produce highly efficient electro-optic modulators [14,15], some other mechanisms dominant during waveguide fabrication at these longer writing wavelengths, could possibly be the cause. One such plausible explanation could be due to the formation of all-optically inverted ferroelectric domains within the illuminated region [16]. The depth of these inverted domains on the + z face at a shorter UV wavelength (244 nm) has been estimated to be of order 30-50 nm. However, the dependence of the depths of such all-optically inverted domain on the writing wavelength has not been studied. The presence of such inverted domains within the waveguide volume will reduce the average phase shift for a given value of the applied voltage which will consequently appear as a reduced EO coefficient. Another possible mechanism which would result in a reduced EO response is damage induced in the crystal by the UV-laser writing step. As the absorption depth for the longer wavelengths is greater, the corresponding damaged volume extends further into the waveguide region, and hence a reduced value for the measured EO coefficient would be obtained for these wavelengths. The UV illuminated tracks were investigated by piezoresponse force microscopy (PFM) in order to identify the cause for the reduction in the EO response. The PFM investigation showed indeed a limited contrast associated with the UV illumination which could be attributed either to a shallow inverted domain or a damaged volume. The PFM results were inconclusive mainly due to the limitation in the depth resolution of the device which is comparable to the dimensions of the waveguiding volume [17].

#117228 - $15.00 USD Received 14 Sep 2009; revised 3 Nov 2009; accepted 3 Nov 2009; published 11 Dec 2009

4. Conclusions

A detailed experimental study on spectral and electro-optic characterization of direct UV-written waveguides in congruent z-cut $LiNbO_3$ crystal has been presented. The waveguides were written with 275, 300.3, 302, and 305 nm wavelengths with various writing powers (35-60 mW) and scan speeds (0.1-1.0 mm/sec). Spectral analysis determined the multimode and single mode wavelength regions, and the cut-off point of the fabricated waveguides. Measurements of cut-off wavelengths of the waveguides for different writing powers and scan speeds confirm the existence of optimum writing conditions for maximum refractive index changes of these waveguides. Changes in cut-off wavelengths of the waveguides with applied uniform electric fields across the substrate indicate that electro-optic response decreases with increasing writing wavelengths. This experimental observation was verified by measuring the mode-widths, mode-depths, and refractive-index contrasts of the waveguides at various applied voltages. Direct measurements of the unclamped electro-optic coefficients (r_{33}) of the waveguides written with different wavelengths were also performed by an interferometric method. It was observed that the r_{33} coefficient is maximum (31 pm/V) for 275 nm writing wavelengths, whereas it is reduced to 14pm/volts for waveguides written with 305 nm writing wavelength. These interferometric measurements have not taken into account the piezoelectric contribution [18] to the phase change of a beam passing through the electro-optic crystal. Nevertheless, this gives a quantitative comparison of the electro-optic coefficients for different waveguides with four different writing wavelengths.

Acknowledgements

We gratefully acknowledge the Royal Society for the International Fellowship of Dr P. Ganguly (No. IIF-2007/R2), the Engineering and Physical Sciences Research Council (EPSRC) for the research funding under grant number EP/C515668, the European Union for funding under the 3-D Demo grant, the Deutsche Forschungsgemeinschaft and the Deutsche Telekom AG. We also acknowledge Prof Karsten Buse and Hendrik Steigerwald for valuable discussions and their support.

#117228 - $15.00 USD Received 14 Sep 2009; revised 3 Nov 2009; accepted 3 Nov 2009; published 11 Dec 2009